The 20th International Conference on
TRANSPORT AND SEDIMENTATION OF SOLID PARTICLES
26–29th September 2023, Wroclaw, Poland

ISSN 0867-7964 ISBN 978-83-7717-392-3

DENSITY WAVE AMPLIFICATION DURING HYDRAULIC TRANSPORT: THE EFFECT OF PIPELINE DESIGN PARAMETERS

Edwin de Hoog[1,2], Arno Talmon[2,3] and Cees van Rhee[2]

DOI: 10.30825/4.14-05.2023

[1]Royal IHC, Smitweg 6, 2961 AW, Kinderdijk, e.dehoog@royalihc.com
[2]Delft University of Technology, Mekelweg 2, 2628CD, Delft
[3]Deltares, Boussinesqweg 1, 2629 HV Delft

ABSTRACT: Pipelines with combined vertical and horizontal pipes can be subject to transient redistribution and accumulation of sediment, also referred to as transient density wave amplification. This process is important to understand for dredging and especially for deep sea mining applications, where a horizontally oriented jumper hose is connected to a long vertical riser. Transient accumulation could ultimately lead to pipeline blockages or pump drive failures. Density wave amplification is partly caused by a velocity difference of particles between horizontal and vertical pipes, and partly by system wide interaction between density waves and the centrifugal pump. Density wave amplification was witnessed at mixture velocities far exceeding the deposit limit velocity (de Hoog et al. 2022), and as such the stability of the pipeline cannot be predicted by designing a pipeline operating point with conventional steady-state design methods. Specifically, the conventional steady-state design methodology only considers steady-state resistance and pump curves to obtain an operating point, and aims to design the operating point above the deposit limit velocity. Transient modeling using 1D Computational Fluid Dynamics (CFD) has shown to be able to predict density wave amplification. In this article the 1D Driftflux model developed by de Hoog et al. (2022) is applied to investigate the influence of system parameters on the rate of density wave amplification. In the simulations the following system parameters are varied: pump drive characteristics, the diameter of the horizontal pipes and the application of flow feedback control.

KEY WORDS: deep sea mining, density waves, vertical hydraulic transport, transient slurry flow, flow assurance, Driftflux

1. INTRODUCTION

Hydraulic transport pipelines are traditionally designed using a steady state methodology. Specifically, the concentration of particles and the pipeline velocity are assumed to be constant in time in space. A steady-state pump curve and resistance curve are computed, and the system operating point results from their intersection (Wilson et al. 2006). The goal of the steady-state design method is to compute an operating velocity above the deposit limit velocity to avoid deposit formation. The deposit limit velocity is

defined as a transitional velocity between suspended flow and flow where particles settle out of suspension and form a bed layer. In case of sliding bed flow, the deposit limit velocity is defined as the transition when the sliding bed stops and becomes stationary.

Experiments in various flow loops with vertical and horizontal sections have shown the unsteady behavior of the slurry. Moreover, particles can redistribute spatially and form highly concentrated density waves that self-amplify. One mechanism of density wave amplification occurs in conjunction with the formation of a bed layer, as particles settle out of suspension, i.e., when the flow velocity falls just below the deposit limit velocity (Matoušek, 1996; Talmon et al., 1999, Talmon et al., 2007). This mechanism is called the "erosion and sedimentation imbalance." Another mechanism occurs at velocities far exceeding the deposit limit velocity and in pipelines with vertical and horizontal sections, combined with particles having significant slip. This mechanism is referred to as "transient accumulation" (de Hoog et al., 2021; de Hoog et al., 2022), see section 3 for more details. Especially, the transient accumulation mechanism forms a large risk for flow continuity, because wave amplification can occur far above the deposit limit velocity. Essentially it can be stated that the steady state design method falls short in these cases.

Because of the unsteady nature of the formation of density waves, and their effect of flow assurance, a 1D CFD Driftflux model was created to predict density wave amplification (de Hoog et al., 2022), to aid in pipeline design. The work of de Hoog et al. (2022) contains the foundation of the 1D Driftflux model, including calibration and validation with experimental data. This article aims to explore mitigation techniques to avoid density wave amplification, using the calibrated 1D Driftflux model.

2. BACKGROUND: THE FREIBERG VERTICAL HYDRAULIC TRANSPORT EXPERIMENTS

Transient accumulation was experienced during a medium scale vertical hydraulic transport testing campaign aimed at studying vertical flows for deep sea mining. The experiments have been described in detail by de Hoog et al. (2022). Other experiments showing density waves were summarized by de Hoog et al. (2021). A short summary of the Freiberg experiments is given in this section.

The Freiberg flow loop had a 121 m vertical riser and a 121 m vertical downgoer. The pipeline diameter was 150 mm. At the top site 57 m of horizontal pipes were required for the pump and separation equipment. A flow meter was placed at the top of the vertical riser, and four pressure sensors at the bottom of the riser and downgoer allowed for a U-loop delivered concentration measurement (Clift & Clift, 1981). The centrifugal pump was outfitted with sensors to measure the manometric pressure p_{man} and pump revolutions n_{pump}. See Figure 1 for a schematic overview of the flow loop.

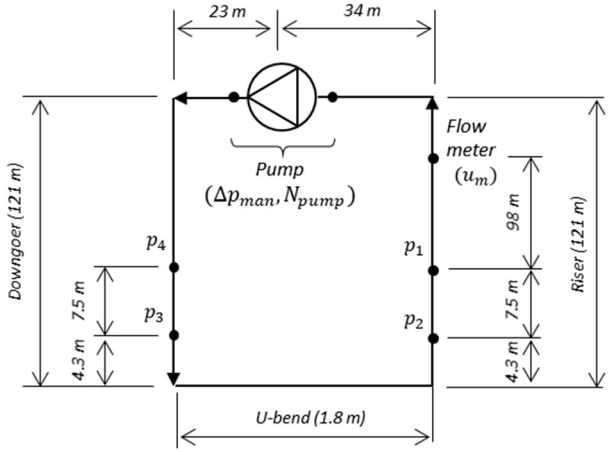

Figure 1 A schematic of the main dimensions and sensor positioning of the Freiberg flow loop.

Experiments were conducted with coarse sand (d_m=741 μm) and medium gravel (d_m=11.2 mm) at volumetric concentrations of 5, 10, 15%. All experiments showed some form of density wave amplification with varying amplification rates, while the pump was running at constant revolutions, and the system operated well above the deposit limit velocity. Coarser particles, higher concentration and lower velocities lead to relatively high amplification rates, compared to smaller particles, lower concentration and higher mixture velocities, respectively.

Figure 2 shows example datasets. For an overview of all experiments, see de Hoog et al. (2022). The deposit limit of the coarse sand was ~2.5 m/s and the gravel ~1.5 m/s. Figure 2 clearly shows that density wave amplification occurs at mixture velocities far exceeding the deposit limit velocity, and during periods where the pump revolutions were stable. How these waves were formed is explained in Section 3.1.

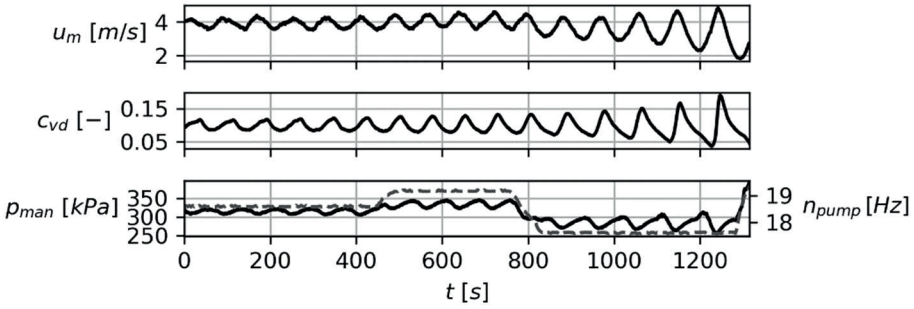

Figure 2 Experimental data time traces of coarse sand, $c = 10\%$. Top: mixture velocity u_m, middle: delivered concentration c_{vd}, bottom: pump manometric pressure p_{man} (solid) and revolutions n_{pump} (dashed).

3. THEORY: TRANSIENT ACCUMULATION AND MITIGATION TECHNIQUES

3.1. TRANSIENT ACCUMULATION

The flow of particles through a pipeline can be modeled using the following 1D transport equation:

$$\frac{\partial c}{\partial t} + \frac{\partial u_s c}{\partial x} = \frac{\partial}{\partial x}\left(\epsilon \frac{\partial c}{\partial x}\right) \tag{1}$$

In Equation 1 c is the concentration, u_s the particle velocity, x the axial coordinate along the pipeline and ϵ an axial diffusion coefficient. Particles travelling upward in a vertical pipe travel faster than in a horizontal pipe of the same diameter. This is due to the stratified nature of flows in horizontal pipes which leads to higher friction compared to vertical flows (de Hoog et al., 2021). Considering only steady-state and no diffusion, Equation 1 becomes:

$$\frac{\partial u_s c}{\partial x} = 0 \tag{2}$$

Thus, the flux $u_s \cdot c$ must remain constant in space between two points:

$$u_{s,1} c_1 = u_{s,2} c_2 \tag{3}$$

Consider a vertical ascending pipe connected to a horizontal pipe, locations (1) and (2), respectively, in Figure 3. The concentration increases between points (1) and (2) equals:

$$\frac{c_2}{c_1} = \frac{u_{s,1}}{u_{s,2}} \tag{4}$$

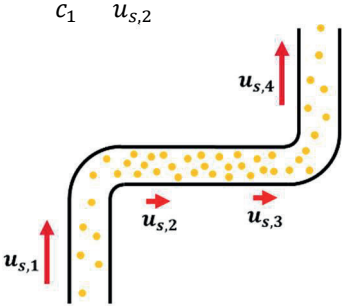

Figure 3 A schematic illustration of the spatial particle concentration distribution and velocity difference between a horizontal and vertical pipe

The particle velocity in vertical pipes can be estimated using the Richardson & Zaki (1954) hindered settling principle:

$$u_s = u_m - v_{ts}(1 - c)^m \tag{5}$$

In Equation 5, v_{ts} is the particle terminal settling velocity and m the Richardson & Zaki (1954) settling parameter are given. In horizontal pipes, using an empirical correlation of the slip ratio:

$$R_s = \frac{u_s}{u_m} \tag{6}$$

The slip ratio model used in the 1D Driftflux mode by de Hoog et al. (2022) was the empirical Sobota & Kril (1992) model.

Consider Figures 3 and 4a, if a density wave flows from a vertical riser into a horizontal pipe (point (1) → (2) in Figure 3), the concentration will increase according to Equation 4 and Figure 4a. If after that the same slurry exited the horizontal pipe and again flowed into a vertical pipe the concentration would recover to its original state. As such, the transient accumulation is temporary. Transient accumulation can however be sustained if the mixture velocity u_m increases while the density wave is flowing through the horizontal pipe. When this wave exits into the second vertical riser, at higher mixture velocity (from point (3) to (4) in Figures 3 and 4a) the recovery of the concentration is less. As such, a net increase in concentration remains. The increase of the mixture velocity occurs, because the density wave exits the vertical pipe and its hydrostatic component no longer needs to be compensated by the centrifugal pump, thus the mixture accelerates.

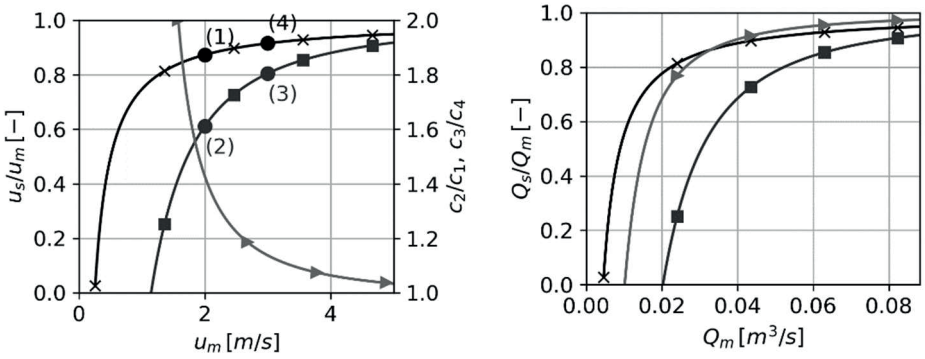

a) x: vertical pipe, square: horizontal pipe, triangle: concentration change of a density wave (right axis)

b) x: vertical pipe, square: horizontal pipe D=150mm, triangle: horizontal pipe D=125mm

Figure 4 (a) An example of the difference in particle velocity and concentration between a 150 mm vertical and a horizontal pipe, using $d_{50} = 11.2\ mm$. (b) An example of the difference in particle flow rate between a 150 mm diameter vertical pipe and a 125 mm horizontal pipe.

3.2. MITIGATION TECHNIQUES

The effect of transient accumulation can be mitigated in three ways, based on the theory explained in Section 3.1. Firstly, by ensuring that the mixture velocity does not change when a density wave exits the vertical pipe, using flow feedback control. This however is an economically expensive solution, since a frequency drive is required to enable control over the pump revolutions. In addition, the pump drive needs a reserve margin in power to prevent the pump drive from operating in a constant power regime, further increasing costs.

A second option is a passive approach, by ensuring that the particle velocity difference between the vertical and horizontal pipe is minimized. This can be achieved by decreasing the horizontal pipe diameter. For example, Figure 4b shows the particle flow rate of a horizontal 125 mm pipe, which matches much better with the particle flow rate of the 150 mm riser, compared to the 150 mm horizontal pipe.

A third option, to reduce density wave amplification, is to design the pipeline such that the centrifugal pump operates at constant power or torque. The constant revolution pump curve is relatively flat, which implies that a small change in pipeline resistance (for instance, a density wave flowing out of a vertical riser) can lead to a large operating point shift. A constant power or torque characteristic is steeper, as such potential changes in operating point are smaller, see Figure 5. A smaller change in the mixture velocity, results in less amplification, according to Figure 4a.

This work aims to study the three methods to mitigate density wave growth as explained above using the 1D Driftflux model developed and validated in de Hoog et al. (2022).

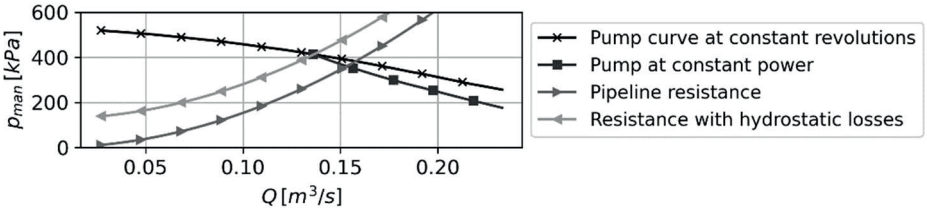

Figure 5 An illustrative example of a small change in pipeline operating point when the pump drive is operating at maximum power, in case of a change in hydrostatic pressure in a pipeline system.

4. 1D DRIFTFLUX MODEL

The mathematical formulation of the 1D Driftflux model is given by Equations 7 and 8. The foundation of the model by de Hoog et al. (2022) is adapted to allow for different cell sizes in the domain (i.e., pipe diameters), which introduces spatial and time derivatives for the cell volume and cross sectional area. Using the finite volume method, the new momentum equation is:

$$\begin{aligned}\frac{\partial}{\partial t}(\rho_m \hat{u}_m V) + \sum_{cell\ faces}(\rho_m \hat{u}_m \hat{u}_m A) = \sum_{cell\ faces}(-pA) - \pi D\tau_m + A\cdot S_p \ldots \\ -\rho_m g A\sin(\omega) + \sum_{cell\ faces}\left[Ac\rho_s(\hat{u}_m - u_s)^2 + A(1-c)\rho_f\left(\hat{u}_m - u_f\right)^2\right]\end{aligned} \tag{7}$$

With ρ_m the mixture density, V the cell volume, A the cell discharge flow area, p the pressure, τ_m the wall shear stress (frictional losses), g the gravitational constant, ω the cell inclination angle ($\omega = 0$ or $\omega = \pm\pi/2$), c the volumetric solids concentration, u_s the particle velocity, u_f the fluid velocity and S_p the pump pressure source term. The mass flow rate mixture velocity is $\hat{u}_m$. The particle transport equation using the finite volume method becomes:

$$\frac{\partial}{\partial t}(cV) + \sum_{cell\ faces} u_s cA = 0 \tag{8}$$

The particle velocity is u_s, which is modelled to have slip relative to the mixture velocity, see de Hoog et al. (2022) for more details. The closure relationships for τ_m, S_p, $u_{s/m}$ and ϵ are explained and validated in de Hoog et al. (2022).

A PID controller can be implemented numerically as follows:

$$U_n = K_P \cdot e_n + \sum_{N=0}^{n} K_I \cdot e_N \Delta t + K_D \cdot \frac{e_n - e_{n-1}}{\Delta t} \tag{9}$$

Where U_n is the controller output at the time step n, K_P the proportional gain constant K_I the integration gain constant, K_D the derivative gain constant and Δt the time step. The error e equals the difference between the mixture velocity at the time step n, $u_{m,n}$, and the controller set point $u_{m,set}$:

$$e = u_{m,n} - u_{m,set} \tag{10}$$

Integration of the error is achieved by summation of all errors of previous time steps, N, and the derivative is computed from the error of the previous time step $n-1$. The controller output is limited to a domain of [-100, 100] and mapped to the drive revolutions in the domain of zero to the maximum drive revolutions [0, $n_{\max}$].

The 1D Driftflux model by de Hoog et al. (2022) contains a centrifugal pump model, furthermore, the pump revolutions were the main input to the 1D model. The pump reference curve in Figure 5 was scaled to the desired revolutions using pump affinity laws. The revolutions of the constant power curve can be computed according to the affinity laws of hydraulic power:

$$n_{cp} = \left(\frac{P_{max} \cdot \eta}{Q \cdot p_{man,cr} \cdot n_{cr}^3} \right)^{\frac{1}{3}} \tag{11}$$

In Equation 11, Q is the volumetric flow rate, n_{cp} is the revolutions of constant power drive at volumetric flow rate Q, P_{max} is the maximum drive power, η the drive efficiency at volumetric flow rate Q, $p_{man,cr}$ the pump manometric pressure at volumetric flow rate Q for a constant revolutions curve and n_{cr} the maximum drive revolutions.

5. SIMULATION RESULTS

The results of the simulation using the three wave mitigation methods as explained in Section 3.2 can be viewed in Section 5. These simulations are the exact same validation simulations as those by de Hoog et al. (2022), using the same settings. The simulations were extended with the density wave mitigation techniques as part of this research.

5.1. DIFFERENTIAL PIPE DIAMETER SIMULATIONS

Figures 6, 7 and 8 show the results of the simulations where the horizontal pipe diameter was reduced from a 6” (150 mm) to a 5” (125 mm) pipe. As such, the particle flow rates of the two pipes are better matched (see Figure 4b). The initial velocity of the 125 mm horizontal pipe was taken from the experimental data (a 150 mm pipe). This results in an even lower velocity in the vertical pipes, and as such the total pressure drop in the system is lower. Therefore, the pump pressure curve was reduced by 5% for these

simulations, to get a similar velocity compared to the experiments. Just as with the simulations in de Hoog et al. (2022), the pump revolutions measured during the experiments were used as input for the model. Another input of the model is u_{crit} (~deposit limit velocity) in the relative velocity model according to Sobota and Kril (1992). The value of u_{crit} in the 125 mm pipe has been scaled according to:

$$\frac{u_{crit,125}}{u_{crit,150}} = \sqrt{\frac{0.125}{0.150}} \tag{12}$$

This scaling follows the Froude number type scale found in most empirical deposit limit velocity models. The simulations show that in two cases (Figure 7 and 8) the wave amplification is reversed and the waves dampen out slowly. The simulation in Figure 6 still shows very slight amplification, but much less than the original case. This solution seems very effective in keeping the flow loop stable.

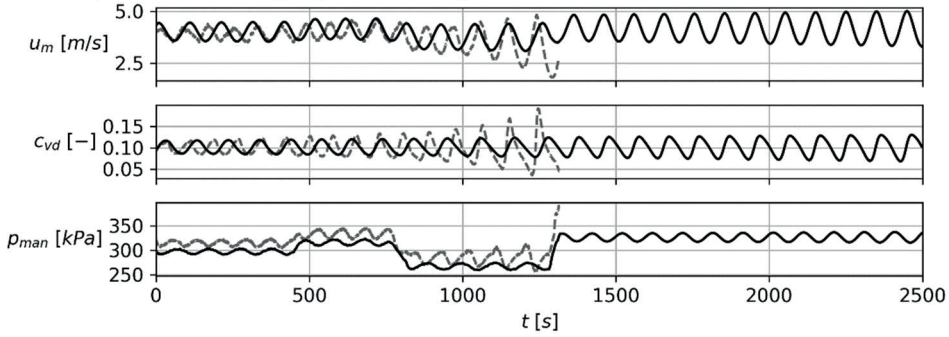

Figure 6 Simulation with a 150mm riser and 125mm horizontal pipes: Coarse sand, $c = 10\%$. Grey (dashed): experimental data. Black (solid): simulation. Source: own study.

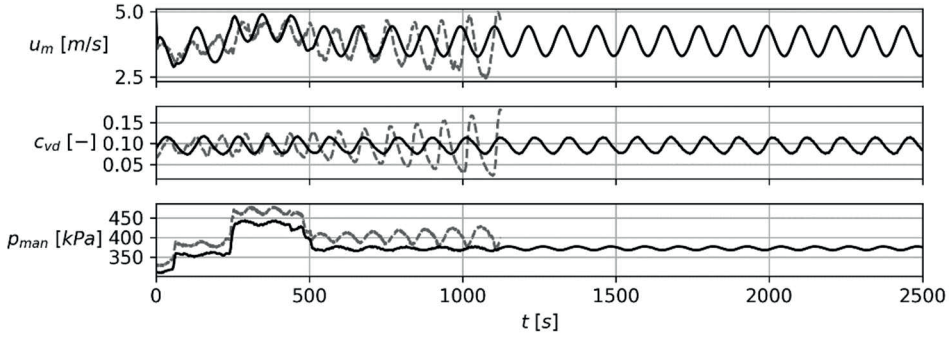

Figure 7 Simulation with a 150mm riser and 125mm horizontal pipes: Medium gravel, $c = 10\%$. Grey (dashed): experimental data. Black (solid): simulation.

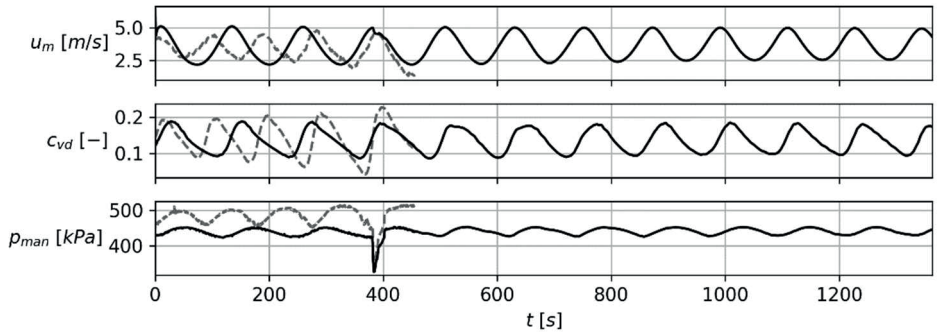

Figure 8 Simulation with a 150 mm riser and 125 mm horizontal pipes: Medium gravel, $c = 15\%$. Grey (dashed): experimental data. Black (solid): simulation.

5.2. CONSTANT POWER DRIVE SIMULATIONS

The simulations in Figures 9, 10 and 11 show the simulation results of using a constant power drive, compared to the original data with a constant revolution drive. Both horizontal and vertical pipes have a diameter of 150 mm. In the original simulation of de Hoog et al. (2022), the measured pump revolutions were used as input for the 1D Driftflux model. However, in these simulations, this cannot be done since the drive is limited by power. As such, the revolutions of the pump are determined by the drive and the load on the drive, see Equation 11. Therefore, the drive power has be chosen such that the initial velocity of the experiment is similar to the simulations of de Hoog et al. (2022).

All three simulations show significantly smaller variations in mixture velocity, which are caused by the constant power drive characteristics (see Figure 5). The rate of amplification of the density wave is less, but amplification has not been mitigated completely. This solution seem only marginally effective.

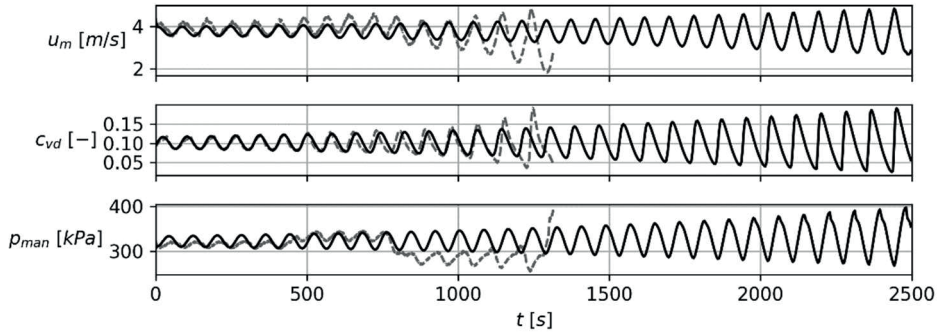

Figure 9 Simulation using a constant power drive: Coarse sand, $c = 10\%$. Grey (dashed): experimental data. Black (solid): simulation. Source: own study.

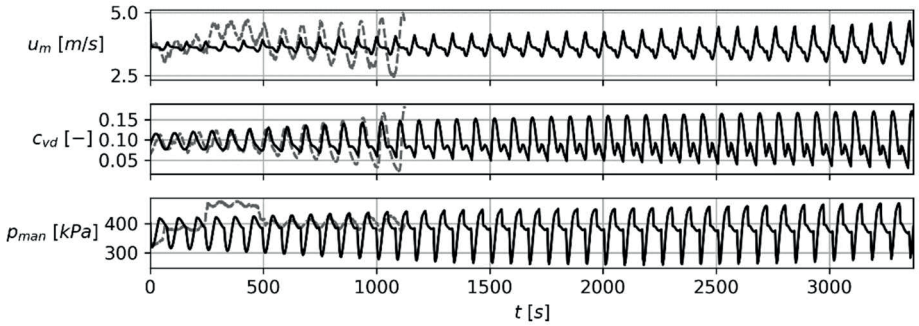

Figure 10 Simulation using a constant power drive: Medium gravel, $c = 10\%$. Grey (dashed): experimental data. Black (solid): simulation. Source: own study.

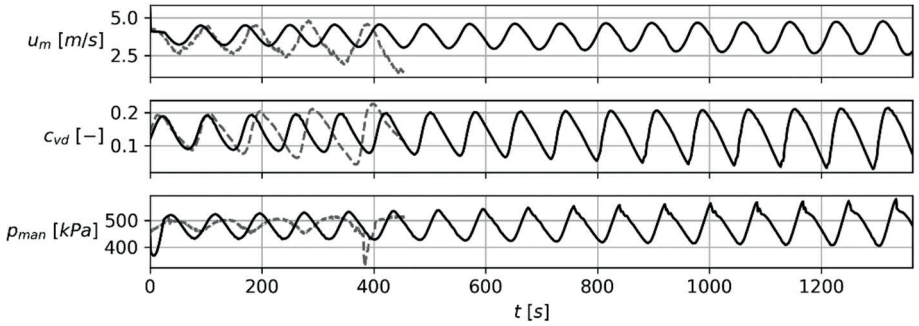

Figure 11 Simulation using a constant power drive: Medium gravel, $c = 15\%$. Grey (dashed): experimental data. Black (solid): simulation.

5.3. SIMULATION USING A PID CONTROLLER FOR STEADY FLOW

The simulations using the PID controller can be viewed in Figures 12, 13 and 14. All pipe diameters are 150 mm. The controller constant was chosen at $K_P = 10000, K_I = 2000, K_D = 0$. The controller is initially disabled, and enabled near the end of the experiment. From this point on the revolutions of the pump is the result of the controller output, evident by the pump manometric pressure. The controller works well to keep the velocity fluctuations to a minimum, and the wave amplification ceases. The density waves in Figure 12 and 13 even dampen out. As such the controller is able to reverse amplification, and maintain a stable transport process. This solution seems very effective, according to the simulations.

6. DISCUSSION AND CONCLUSIONS

Transient accumulation can be mitigated using three techniques, as shown by 1D CFD simulations in this article. The first technique is to reduce the pipe diameter of the horizontal sections. This diminishes the mismatch in particle velocity between the riser and the horizontal pipes. Two out of three simulations showed that this passive design technique can lead to damping of the density waves, and the other simulation showed that

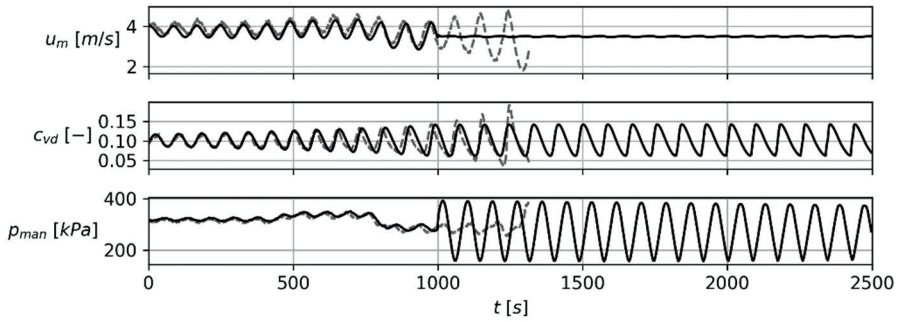

Figure 12 Simulation using a PID controller: Coarse sand, $c = 10\%$. Grey (dashed): experimental data. Black (solid): simulation.

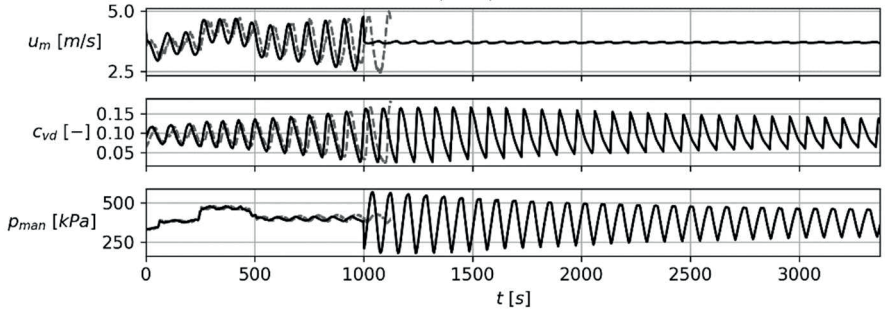

Figure 13 Simulation using a PID controller: Medium gravel, $c = 10\%$. Grey (dashed): experimental data. Black (solid): simulation.

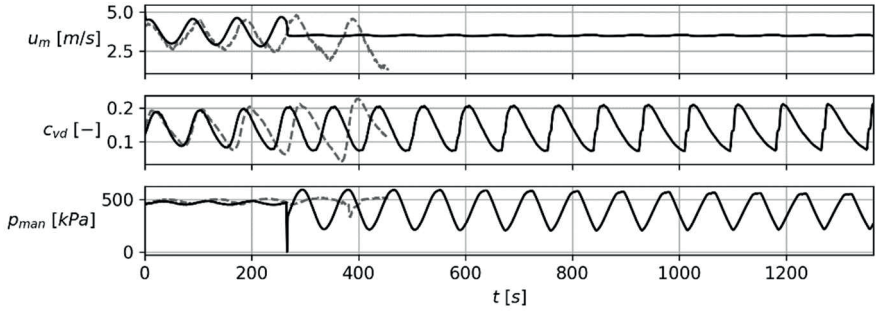

Figure 14 Simulation using a PID controller: Medium gravel, $c = 15\%$. Grey (dashed): experimental data. Black (solid): simulation.

the waves did not grow further. The second technique is to use a constant power drive, with the idea to reduce the mixture velocity fluctuations caused by the density waves. This technique works as theorized, but is not able to completely reverse amplification like the first technique. The third technique is to use a PID controller to maintain a steady mixture velocity. This is by far the most effective solution, however this is also the most economically expensive, as this requires an overpowered drive (to allow for revolution

control) and a frequency controller. Designing the controller and choosing the correct drive power can be done well using simulations, by simulating large waves and designing the controller to cope with the waves.

Passive density wave mitigation techniques are changing the pipe diameter of horizontal sections, and designing the pump drive in a constant power range (however then PID control is not possible). Matching particle flow rate by changing the pipe diameter, is the most effective of the passive methods, however not as effective as PID control. If a passive density wave mitigation design is desired combining the two passive techniques mentioned above will yield the best result. The advantage is that both passive methods can be designed for steady state calculations (Figures 6 and 7), therefore the pipeline designer does not need to carry out 1D simulations. However, to know how effective these two solutions are for a certain pipeline system, still requires doing 1D simulations.

ACKNOWLEDGEMENTS

This research is funded by Royal IHC and TKI Martitiem. A very special thanks need to go to Cees van Rhee, full professor in Dredging Engineering. As a pioneer he introduced us into the exciting topic of deep-sea mining. Cees unexpectedly passed away at the age of 64. We will remember him as a dear colleague and inspiring mentor.

REFERENCES

1. Clift, R., Clift, D.H. 1981. Continuous measurement of the density of flowing slurries. *Int. J. Multiphase Flow* 7(5), pp. 555-561.
2. de Hoog, E., van Wijk, J.M., Talmon, A.M., van Rhee, C. 2022. Predicting density wave amplification of settling slurries using a 1D Driftflux model. *Powder Technology* 400 (3), 117252
3. de Hoog, E., Talmon, A.M., van Rhee, C. 2021. Unstable transients affecting flow assurance during hydraulic transportation of granular two phase slurries, *Journal of Hydraulic Engineering* 147 (9), pp. 1–12
4. Matoušek V. 1996. Unsteady solids flow in a long slurry pipeline with pumps in series – process of material aggregation. *Journal of Hydrology and Hydromechanics* 44 (6), pp. 396–409.
5. Richardson, J.F. and Zaki, W.N. 1954. Sedimentation and fluidisation: Part i. *Transactions 699 Institution of Chemical Engineers* 32, pp. 35.
6. Sobota, J., Kril, S.I. 1992. Liquid and solid velocity during mixture flow. *In Proceedings of the 10th Int. Kolloquium massenguttransport durch rohrleitungen*. Univ. GH-Paderborn, 20-22 May 1992, Meschede, Germany.
7. Talmon, A.M. 1999. Mathematical analysis of the amplification of density variations in long-distance sand transport pipelines, *In Proceedings of the 14th Int. Conf. on Slurry Handling and Pipeline Transport*, 8-10 September 1999, Maastricht, the Netherlands, pp. 3–20.
8. Talmon, A.M., Aanen, L., Bakker-Vos, R. 2007. Laboratory tests on self-excitation of concentration fluctuations in slurry pipelines, *Journal of Hydraulic Research* 45 (5), pp. 653–660.
9. Wilson et al. 2006 - *Slurry Transport Using Centrifugal Pumps*. Ed. 3. US: Springer US.